

# Preparation and Characterization of Polyimide/Al<sub>2</sub>O<sub>3</sub> Hybrid Films by Sol–Gel Process

Pengchang Ma,<sup>1</sup> Wei Nie,<sup>1</sup> Zhenghua Yang,<sup>1</sup> Peihong Zhang,<sup>2</sup> Gang Li,<sup>2</sup> Qingquan Lei,<sup>2</sup> Lianxun Gao,<sup>1</sup> Xiangling Ji,<sup>1</sup> Mengxian Ding<sup>1</sup>

<sup>1</sup>Laboratory of Polymer Engineering and State Key Laboratory of Polymer Physics and Chemistry, Changchun Institute of Applied Chemistry, Graduate School of the Chinese Academy of Sciences, Chinese Academy of Sciences, Changchun 130022, People's Republic of China

<sup>2</sup>Electrical and Electronic Engineering College, Harbin University of Science and Technology, Harbin 150040, People's Republic of China

Received 13 May 2007; accepted 4 September 2007

DOI 10.1002/app.27540

Published online 11 January 2008 in Wiley InterScience (www.interscience.wiley.com).

**ABSTRACT:** A sol–gel process has been developed to prepare polyimide (PI)/Al<sub>2</sub>O<sub>3</sub> hybrid films with different contents of Al<sub>2</sub>O<sub>3</sub> based on pyromellitic dianhydride (PMDA) and 4,4'-oxydianiline (ODA) as monomers. FESEM and TEM images indicated that Al<sub>2</sub>O<sub>3</sub> particles are relatively well dispersed in the polyimide matrix after ultrasonic treatment of the sol from aluminum isopropoxide and thermal imidization of the gel film. The dimensional stability, thermal stability, mechanical properties of hybrid PI films were improved obviously by an addition of adequate Al<sub>2</sub>O<sub>3</sub> content, whereas, dielectric property and

the elongation at break decreased with the increase of Al<sub>2</sub>O<sub>3</sub> content. Surprisingly, the corona-resistance property of hybrid film was improved greatly with increasing Al<sub>2</sub>O<sub>3</sub> content within certain range as compared with pure PI film. Especially, the hybrid film with 15 wt % of Al<sub>2</sub>O<sub>3</sub> content exhibited obviously enhanced corona-resistance property, which was explained by the formation of compact Al<sub>2</sub>O<sub>3</sub> network in hybrid film. © 2008 Wiley Periodicals, Inc. *J Appl Polym Sci* 108: 705–712, 2008

**Key words:** polyimide film; alumina; sol–gel process

## INTRODUCTION

Polyimides have been extensively applied in the fields of microelectronics and aerospace industries as a material for electronic packaging and electrical insulating due to its high thermal stability, outstanding dimensional stability, excellent mechanical properties, and low dielectric constant in a considerably wide temperature range.<sup>1–10</sup> With the development of advanced industry, polyimide materials with special functions are required to be developed.

In recent years, polyimide hybrid materials have attracted much attention due to improved properties

than their virgin state, such as in thermal property, mechanical property, corona-resistance property, and other special properties by an introduction of small amount of inorganic compounds. Generally, polyimide hybrid films are obtained by sol–gel route,<sup>11–22</sup> intercalation approach,<sup>23–25</sup> and blending method.<sup>26–33</sup> Intercalation approach, generally reversible, that involves the introduction of a guest species into a host structure without a major structural modification of the host. In the strictest sense, intercalation refers to the insertion of a guest into a two-dimensional host; however, the term also now commonly refers to one-dimensional and three-dimensional host structures. Several strategies, such as *in situ* intercalation polymerization, exfoliation adsorption and melt intercalation, have been developed to fabricate polymer/inorganic materials nanocomposites. Among these strategies, the melt intercalation is attractive because of its versatility, its compatibility with current polymer processing techniques, and its environmentally benign character due to the absence of solvent. Compared to the intercalation approach, sol–gel processing can offer an advantage for making materials at lower temperatures because precursors are mixed in the right proportion at the very beginning of the process, i.e., in solution. And the sol–gel process includes hydrolysis of alkoxides, followed by polycondensation of the hydrolyzed intermediates.

Correspondence to: X. Ji (xlji@ciac.jl.cn) or M. Ding (mxding@ciac.jl.cn).

Contract grant sponsors: National Science and Technology Committee, the National Natural Science Foundation of China; contract grant numbers: 20674085, 50633030, 50621302.

Contract grant sponsor: "863" Project; contract grant number: 2006AA03Z224.

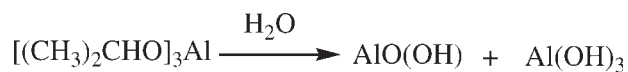
Contract grant sponsor: Distinguished Young Fund of Jilin Province; contract grant number: 20050104.

Contract grant sponsor: Chinese Academy of Sciences; contract grant number: KJCX2-SW-H07.

Contract grant sponsor: International Collaboration Project; contract grant numbers: 04-03GH268, 20050702-2.

*Journal of Applied Polymer Science*, Vol. 108, 705–712 (2008)

© 2008 Wiley Periodicals, Inc.



**Scheme 1** Hydrolysis of AIP.

Its unique low-temperature processing characteristics provide unique opportunities to prepare polyimide hybrid materials. Many polyimide hybrid materials were prepared by sol-gel process, using  $\text{Si}(\text{OR})_4$  or  $\text{Ti}(\text{OR})_4$  as starting materials, whereas, aluminum alkoxides have been less reported in literature, although they exhibit potential applications in many fields, such as in varnishes, textile impregnation, cosmetics, and as an intermediate in pharmaceutical production.<sup>34</sup> The obtained aluminum oxide ( $\text{Al}_2\text{O}_3$ ) is an interesting material in electrical, engineering, and biomedical areas.

Here, we report the preparation of polyimide- $\text{Al}_2\text{O}_3$  composite films by sol-gel route and *in situ* polymerization using aluminum alkoxides as starting materials and insoluble polyimide as the matrix. Finally, the PI/ $\text{Al}_2\text{O}_3$  hybrids based on ODA and PMDA were obtained with different content of  $\text{Al}_2\text{O}_3$  nanoparticles. The related properties and morphologies of the hybrid films are investigated.

## EXPERIMENTAL

### Materials

PMDA (pyromellitic dianhydride) and ODA (4,4'-oxydianiline) were prepared from our laboratory and purified by sublimation under reduced pressure. Their chemical structures are shown in Scheme 2. Aluminum isopropoxide (AIP) (98%) and 3-aminopropyltriethoxysilane were purchased from ACROS. *N,N*-dimethyl acetyamide (DMAc) as a solvent was freshly distilled from phosphorus pentoxide. Acetyl acetone was used as received commercially and dried with molecular sieve before using.

### Preparation of polyimide/ $\text{Al}_2\text{O}_3$ hybrid films

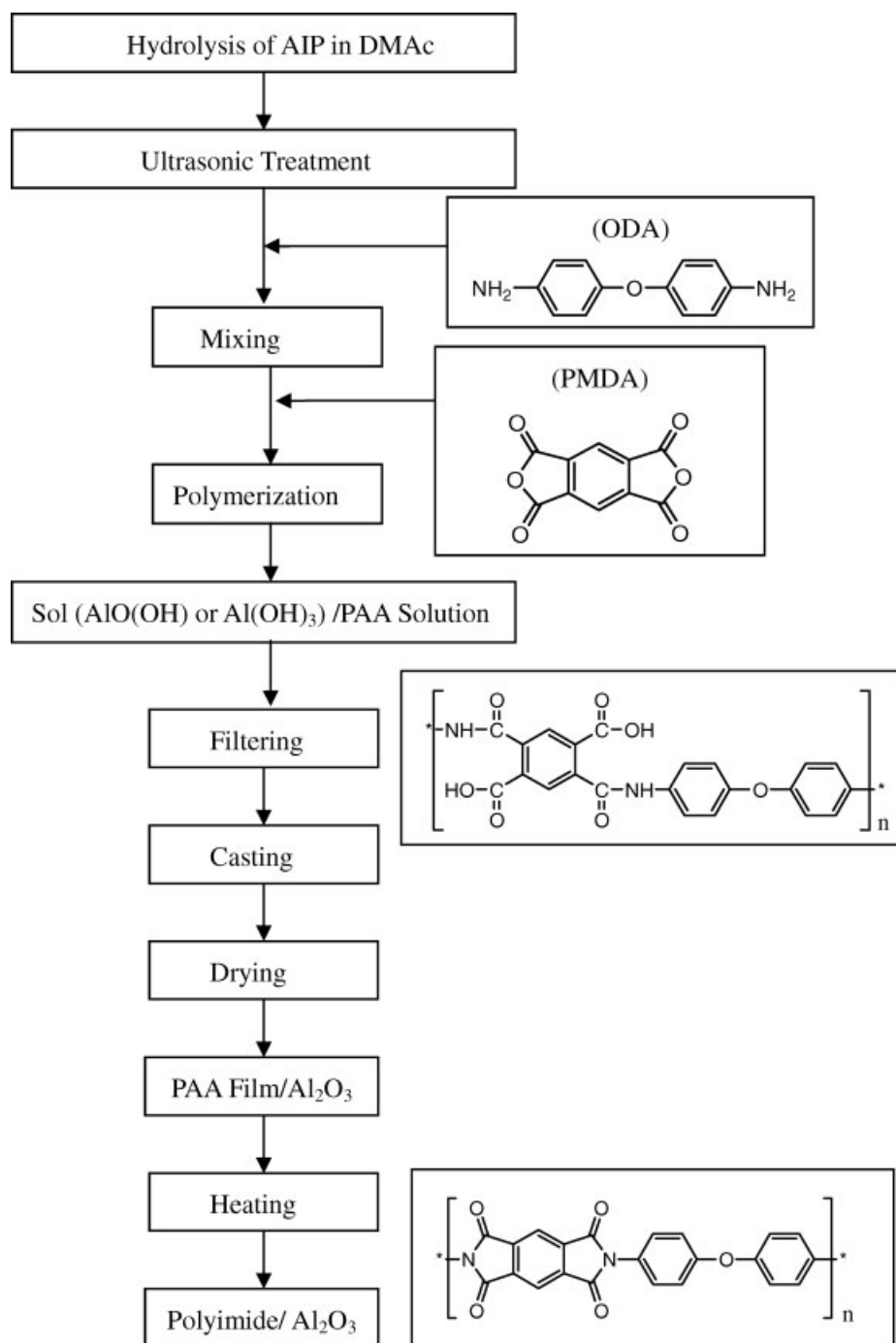
The sol ( $\text{Al}(\text{OH})$  or  $\text{Al}(\text{OH})_3$ )/poly(amic acid) was prepared by sol-gel process (see Scheme 1) and *in situ* polymerization with the procedure as shown in Scheme 2. In a typical experiment, 5.21 g of AIP powder was added into 70 mL of DMAc and then was added proper deionized  $\text{H}_2\text{O}$ , then 0.079 g 3-aminopropyltriethoxysilane was added into the resultant solution, followed by ultrasonic treatment to get homogeneous sol.<sup>32</sup> Then, 6.00 g of ODA (0.03 mol) was added to the above solution under a nitrogen atmosphere. After ODA was completely dissolved, 6.54 g of PMDA (0.03 mol) and additional 50.6 mL of DMAc were added. The mixture was

stirred at room temperature for 12 h under a nitrogen atmosphere to give a homogeneous and viscous sol/poly(amic acid) solution with a concentration of 10% poly(amic acid) in DAMc. After filtration of above solution with a funnel of 30–50  $\mu\text{m}$  pore size, the solution was cast onto a glass substrate and followed by air-drying for 2 h at 60°C. The resultant gel film was cured through a heating at a rate of 2.5°C/min from room temperature to 200°C and holding at 200°C for 1 h, then heating at the same rate to 430°C and holding for 1 h to make the sol completely decompose. Finally, the PI hybrid film was obtained after the cooled film peeled off from the glass substrate by immersion into warm water.

A series of PI hybrid film with the  $\text{Al}_2\text{O}_3$  content of 0, 2.5, 5, 10, 12.5, 15, 20 wt %, respectively, was prepared in the similar procedure. The films were  $\sim 31 \pm 2 \mu\text{m}$  in thickness.

### Measurements

Aluminum contents were determined by inductively coupled plasma (ICP) using a POEMS spectrometer. FTIR spectra of films were obtained with a BRUKER Vertex 70 FTIR spectrometer. Field emission scanning electron micrographs (FESEM) were performed on a XL-30 scanning electron microscope using fractured film samples in liquid nitrogen. For FESEM measurement, polyimide and hybrid films were immersed in liquid nitrogen for 2 min, then were fractured very quickly. Transmission electron microscopy (TEM) images were taken using a JEOL-JEM 1010 instrument operated at 120 kV. The coefficient of the linear thermal expansion was obtained by thermal mechanical analysis (TMA), and data was recorded on a TMA V2.1 Dupont 9900 with a rectangular film specimen (5 mm wide and 30 mm long) at a heating rate of 5°C/min. Dynamic mechanical analysis (DMA) was carried out in tension mode with a DMTA V (Rheometric Scientific<sup>TM</sup>) with a rectangular film specimen (5 mm wide and 30 mm long) at a heating rate of 5°C/min. The temperature dependence of the storage modulus ( $E'$ ) and  $\tan \delta$  was measured at a frequency of 1 Hz, with an initial longitudinal tension of 0.5 N applied to the samples. Mechanical properties were measured on Instron 1121 with 500 mm  $\times$  5 mm specimens at a drawing rate of 50 mm/min, and gauge length is 20 mm. The dielectric constant was tested on a CCJ-1B capacitance meter with a two-electrode system. The corona-resistance property was measured by using CS2674C pressure-resistant meter under a voltage of 3 kV. Solution viscosity of the sol ( $\text{Al}(\text{OH})$  or  $\text{Al}(\text{OH})_3$ )/poly(amic acid) was measured using a rotary viscometer with a 10 wt % of poly(amic acid) in DMAc solution at  $30 \pm 0.1^\circ\text{C}$ .



Scheme 2 Schematic of Al<sub>2</sub>O<sub>3</sub>/polyimide hybrid films.

## RESULTS AND DISCUSSION

### Synthesis of polyimide/Al<sub>2</sub>O<sub>3</sub> hybrid films

Aluminum alkoxides are generally used as Al<sub>2</sub>O<sub>3</sub> source in sol-gel reactions and aluminum isopropoxide is one of the widely used precursors. In our initial experiment, aluminum tri-butoxide was used as a precursor to Al<sub>2</sub>O<sub>3</sub> in hybridization. When it was dropped into the solution of poly(amic acid), aggregation occurred and lumps formed quickly, which

could not be dispersed by vigorous stirring. The main reason is due to aluminum alkoxides with very high reaction actives, which results in fast hydrolysis and strong interaction of the resultant sol with polymer. There are two methods to solve above aggregation. One method is to add dispersant to make the sol homogenously, but the experiments showed a bad effect to prevent aggregation. The other is to exploit ultrasonicator to reach a homogeneous sol. Definitely, the second approach exhibits a good

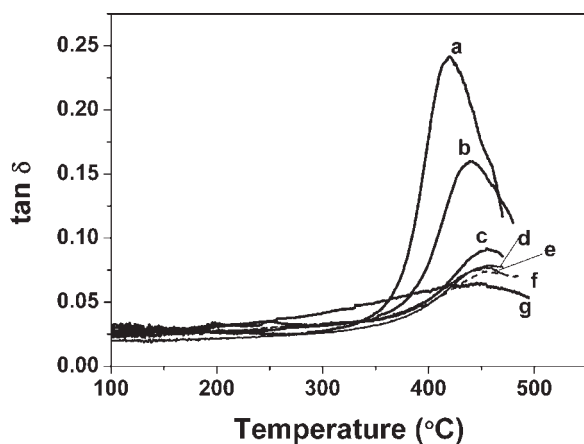


**Figure 1** Spectra of  $\tan \delta$  for pure PI and the hybrid films (a) 0%, (b) 2.5%, (c) 5%, (d) 10%, (e) 12.5%, (f) 15%, (g) 20%.

result. After the sol solution was treated by an ultrasonicator, ODA was added and dissolved completely in DMAc. Then, PMDA was added stepwise to polycondense with the ODA to produce a homogenous and viscous solution. The rotary viscosity of the above solution was in the range of 500–600 poise at 30°C. Then, the solution was filtrated and cast on a glass substrate and followed by drying to get a self-supported gel film. Finally, the gel film was treated at high temperature, and the PI/Al<sub>2</sub>O<sub>3</sub> hybrid films with different Al<sub>2</sub>O<sub>3</sub> content were obtained.

### Thermal properties

Figure 1 illustrates the temperature dependence of the  $\tan \delta$  for pure PI film and hybrid films. The maxima reflect glass transition ( $T_g$ ) for PI matrix. They are located at 420, 441, 455, 458, 455, 454, and 444°C, corresponding to the Al<sub>2</sub>O<sub>3</sub> contents of 0, 2.5, 5, 10, 12.5, 15, and 20%, respectively. It seems that the movement of polyimide molecular chains is confined in the rigid Al<sub>2</sub>O<sub>3</sub> network structure, which makes the  $T_g$  increase about 20–40°C. When the Al<sub>2</sub>O<sub>3</sub> content is in the range 5–15%, the  $T_g$  of the hybrid films almost keeps at a constant level. Whereas the hybrid film with 20% of Al<sub>2</sub>O<sub>3</sub>, the  $T_g$  decreased abruptly but is still higher than that of pure PI film. It is attributed to a local aggregation of Al<sub>2</sub>O<sub>3</sub> particles.

Thermal stability of the hybrid films was evaluated from TGA curves in Figure 2. The pure PI film gives the decomposition temperatures of 575°C at 5% weight loss under an air atmosphere. However, increasing Al<sub>2</sub>O<sub>3</sub> composition, the  $T_5$  is enhanced to 587, 590, 595, 597, 601°C corresponding to Al<sub>2</sub>O<sub>3</sub> content of 2.5, 5, 10, 12.5, 15%, respectively. With further increase of Al<sub>2</sub>O<sub>3</sub> content to 20%, a slight decrease in  $T_5$  at 592°C was detected. The

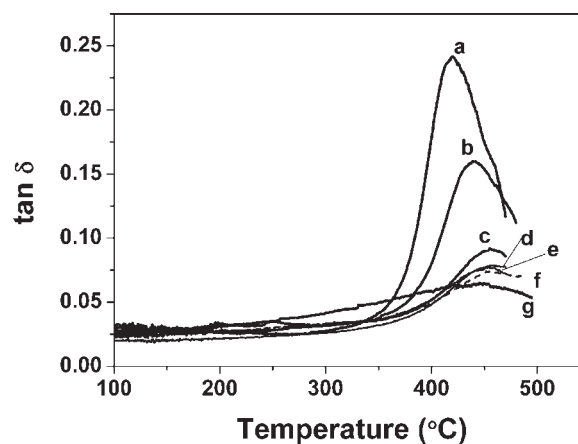


**Figure 2** TGA curves of PI/Al<sub>2</sub>O<sub>3</sub> hybrid films (a) 0%, (b) 2.5%, (c) 5%, (d) 10%, (e) 12.5%, (f) 15%, (g) 20%.

above results indicate that the thermal stability of pure PI film could be improved by an addition of Al<sub>2</sub>O<sub>3</sub> particles.

### Mechanical properties

The mechanical properties of the PI/Al<sub>2</sub>O<sub>3</sub> hybrid films are listed in Table I. We found that the Young's moduli of the hybrid films increase with Al<sub>2</sub>O<sub>3</sub> content. For example, the Young's modulus for pure PI film is 3.20 GPa. As the film incorporated with 2.5 wt % of Al<sub>2</sub>O<sub>3</sub>, the Young's modulus slightly increased to 3.38 GPa. When the Al<sub>2</sub>O<sub>3</sub> content further increased to 12.5%, the Young's modulus markedly increased to 4.26 GPa, which is 33.2% higher than the pure PI film. The increase in the Young's modulus reflects the reinforcement effect of Al<sub>2</sub>O<sub>3</sub> particles in the composites, which is popular in composite materials. The tensile strength and elongation at break for the pure film are 265 MPa and 60.1%, respectively. As the film includes 2.5 wt % of Al<sub>2</sub>O<sub>3</sub>, the tensile strength and elongation at break decreased to 201.7 MPa and 45.7%, respectively. Further increase in the Al<sub>2</sub>O<sub>3</sub> content leads to a gradual decrease in the tensile strength and the elongation at break, which is probably caused by the

**TABLE I**  
Mechanical Properties of PI/Al<sub>2</sub>O<sub>3</sub> Hybrid Films

Al <sub>2</sub> O <sub>3</sub> (wt %)	Tensile modulus (GPa)	Tensile strength (MPa)	Elongation (%)
0	3.20	265	60.1
2.5	3.38	202	45.7
5	3.57	196	24.5
10	3.96	185	19.9
12.5	4.26	175	12.7
15	4.40	168	9.34
20	4.57	40.4	1.12



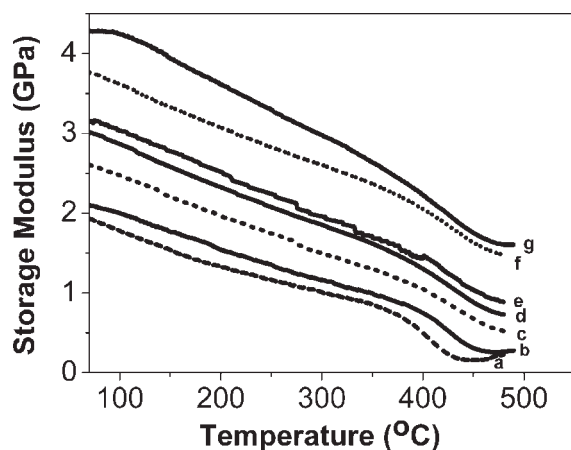


**Figure 3** Dynamic mechanical spectra ( $E'$ ) for pure PI and the hybrid films (a) 0 %, (b) 2.5 %, (c) 5%, (d) 10%, (e) 12.5%, (f) 15%, (g) 20%.

partial aggregation of the Al<sub>2</sub>O<sub>3</sub> particles in PI matrix. When the Al<sub>2</sub>O<sub>3</sub> content is no more than 15%, the PI hybrid films still exhibit good mechanical properties. However, as the Al<sub>2</sub>O<sub>3</sub> content increased to 20%, the tensile strength and elongation at break of the films decreased dramatically to 40.4 MPa and 1.1%, respectively. On the one hand, the sol-gel reaction happened simultaneously with polymerization, possibly the average molecular weight of PI matrix was influenced by a formation of alumina. On the other hand, more alumina content readily leads to a serious aggregation of Al<sub>2</sub>O<sub>3</sub> particles.

The storage modulus ( $E'$ ) of hybrid films increased remarkably with the increase of Al<sub>2</sub>O<sub>3</sub> content in the range of 70–480°C as shown in Figure 3. The  $E'$  value of pure PI film decreased slowly from 1.93 GPa at 70°C to 0.63 GPa at 380°C while it declined dramatically only in excess of 380°C and then displayed a minimum at about 450°C. PI/Al<sub>2</sub>O<sub>3</sub> hybrid

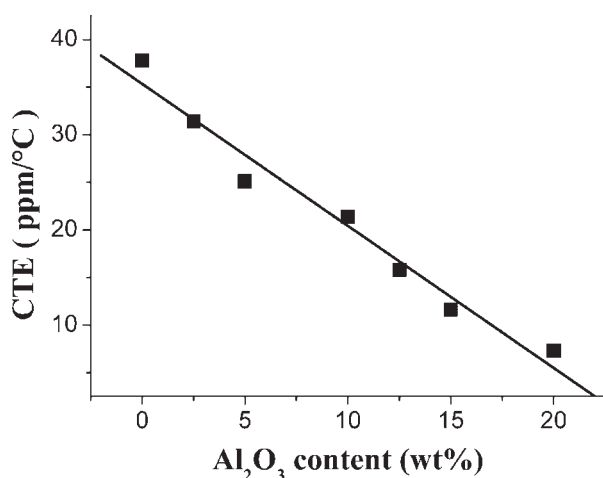


**Figure 4** Relationship between CTE of hybrid films and Al<sub>2</sub>O<sub>3</sub> content.

films also show a decreased modulus with temperature, but no minimum was observed. The starting storage moduli of hybrid films are of 2.11, 2.61, 3.01, 3.15, 3.76, 4.25 GPa corresponding to 2.5, 5, 10, 12.5, 15, 20% of Al<sub>2</sub>O<sub>3</sub> particles. It should be mentioned that hybrid films with 15 and 20% of Al<sub>2</sub>O<sub>3</sub> still possess high storage modulus of 1.48 and 1.60 GPa at about 480°C, implying a good dynamic mechanical property that is important for its applications in high-temperature range. However, increasing Al<sub>2</sub>O<sub>3</sub> content gives rise to an increase of  $E'$  values, which resulted from an addition of rigid Al<sub>2</sub>O<sub>3</sub> network to make the segmental mobility of PI chains difficult in the composites.

### Dimensional stability

It is well known that good dimensional stability is very important in a broad temperature range for microelectronic industry and space applications. Generally, addition of inorganic particles or compounds can improve the dimensional stability of composites to some extent. As reported in literature for PI/Al<sub>2</sub>O<sub>3</sub> system, the hybrid film with 20 wt % of Al<sub>2</sub>O<sub>3</sub> has a coefficient of thermal expansion (CTE) of 31.6 ppm/°C, 15% lower than pure PI film.<sup>24</sup> In Figure 4, we can find that the CTE of the PI hybrid films decreases gradually with the Al<sub>2</sub>O<sub>3</sub> content as shown in Table II. The hybrid film with 12.5 wt % of Al<sub>2</sub>O<sub>3</sub> has a CTE of 15.8 ppm/°C in the range of 50–350°C, only 41.8% of that of pure PI film. As the Al<sub>2</sub>O<sub>3</sub> content increased to 20%, CTE of hybrid film further decreased to 7.3 ppm/°C, only 19.3% of that of PI film. Intriguingly, an excellent linear relationship can be found in Figure 4 between the CTE values and the alumina content, which indicates that dimensional stability of the PI film could be improved obviously by incorporation of Al<sub>2</sub>O<sub>3</sub> particle through the above sol-gel route.

### Electrical property

A phenomenon generally known as “corona” that could cause ionization in the insulating layer is recognized as the major reason for electric breakdown

**TABLE II**  
Thermal Properties of PI/Al<sub>2</sub>O<sub>3</sub> Hybrid Films

Al <sub>2</sub> O <sub>3</sub> (wt %)	Decomposition temperature $T_5$ (°C)	CTE (ppm/°C)	$T_g$ (°C)
0	575	37.8	430
2.5	587	31.4	451
5	590	25.1	465
10	595	21.4	468
12.5	597	15.8	465
15	601	11.6	464
20	592	7.3	444

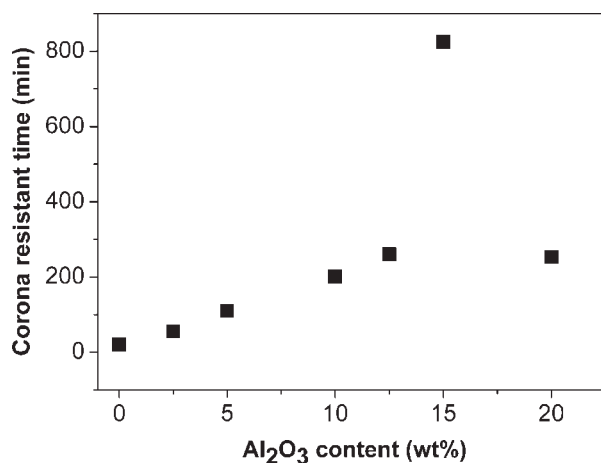


**Figure 5** Corona resistance time of PI/Al<sub>2</sub>O<sub>3</sub> hybrid films in the electrical aging.

of an insulation material when the voltage stress reached a critical level. Draper et al. reported that the polyimide films with addition of some ultrafine inorganic additives exhibited good corona-resistance property.<sup>35</sup> And of all the film materials, only KAPTON@CR manufactured by Dupont exhibited the best corona-resistance property. Figure 5 shows the time to failure for PI hybrid films in electrical aging test, which was determined by the breakdown time of the films under a highly constant voltage. The PI hybrid films show evidently improvement in electrical aging performance as compared with pure PI film. Surprisingly, the hybrid PI film with 15 wt % of Al<sub>2</sub>O<sub>3</sub> exhibits a significant enhancement, i.e., the time to failure in electrical aging at 3 kV is 825 min, which is 55 times longer than that of pure PI film. Definitely, the addition of Al<sub>2</sub>O<sub>3</sub> gave rise to the structural change in composites. As we know, the Al—O bond energy is higher than that of C—C, C—H, C—O bond, the addition of Al<sub>2</sub>O<sub>3</sub> made the

composite surface ionization difficult, and FTIR spectra (see Fig. 7) indicate the O···H···O bonds formed between alumina and PI molecules in the composites. When the Al<sub>2</sub>O<sub>3</sub> content is no more than a certain value, the Al<sub>2</sub>O<sub>3</sub> particles could be well dispersed in the polyimide matrix to enhance the corona-resistance performance. As the Al<sub>2</sub>O<sub>3</sub> content exceeds a certain value, Al<sub>2</sub>O<sub>3</sub> particles are dispersed heterogeneously and it will lead to a decrease in the corona-resistance property. The hybrid film containing 20% Al<sub>2</sub>O<sub>3</sub> content confirms this hypothesis.

Figure 6 shows the permittivity of the PI hybrid films at different Al<sub>2</sub>O<sub>3</sub> content. It can be seen that the permittivity was slightly increased at first with the Al<sub>2</sub>O<sub>3</sub> content and then increased dramatically as the Al<sub>2</sub>O<sub>3</sub> content is more than 12.5% at frequency of 10<sup>2</sup> Hz. The hybrid film with 12.5% of Al<sub>2</sub>O<sub>3</sub> shows the permittivity of 3.5, which is about 13% higher than that of PI film (3.1). As the Al<sub>2</sub>O<sub>3</sub> content increased to 15 and 20%, the permittivity increased to 4 and 4.4 at the same frequency. Generally, for the samples less than 12.5% of Al<sub>2</sub>O<sub>3</sub> content, the permittivity decreased slightly as the frequency increased. It should be mentioned that the samples with 15 and 20% of show a dramatic decrease in permittivity with the frequency. Possibly, too high Al<sub>2</sub>O<sub>3</sub> content results in heterogeneously dispersion of Al<sub>2</sub>O<sub>3</sub> particles in the PI matrix.

### Component, structure, and morphology

Component analysis for hybrid films using ICP showed that the Al<sub>2</sub>O<sub>3</sub> content is close to the calculated values. For example, the Al<sub>2</sub>O<sub>3</sub> content from ICP is 10.5 wt %, close to the theoretical value 10 wt %. The result indicated the aluminum precursor transferred into Al<sub>2</sub>O<sub>3</sub>. This result was also confirmed by FTIR spectra in Figure 7. Figure 7(a) is

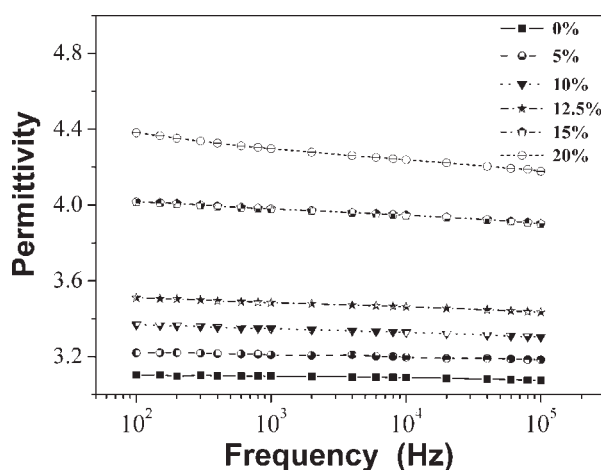


**Figure 6** Effect of Al<sub>2</sub>O<sub>3</sub> content on permittivity of the hybrid films.

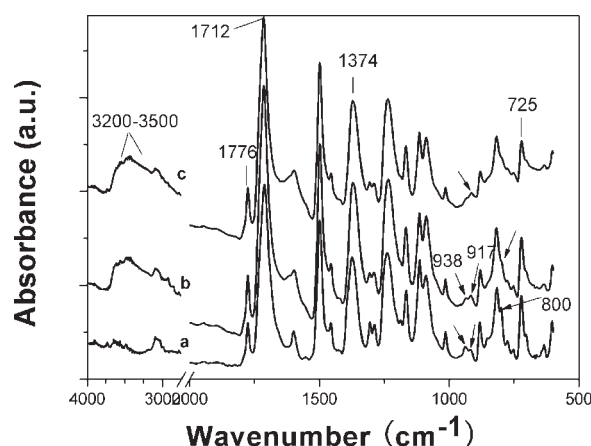


**Figure 7** FTIR spectra of (a) polyimide film, (b, c) polyimide/Al<sub>2</sub>O<sub>3</sub> with the Al<sub>2</sub>O<sub>3</sub> content of 5 and 15%, respectively.

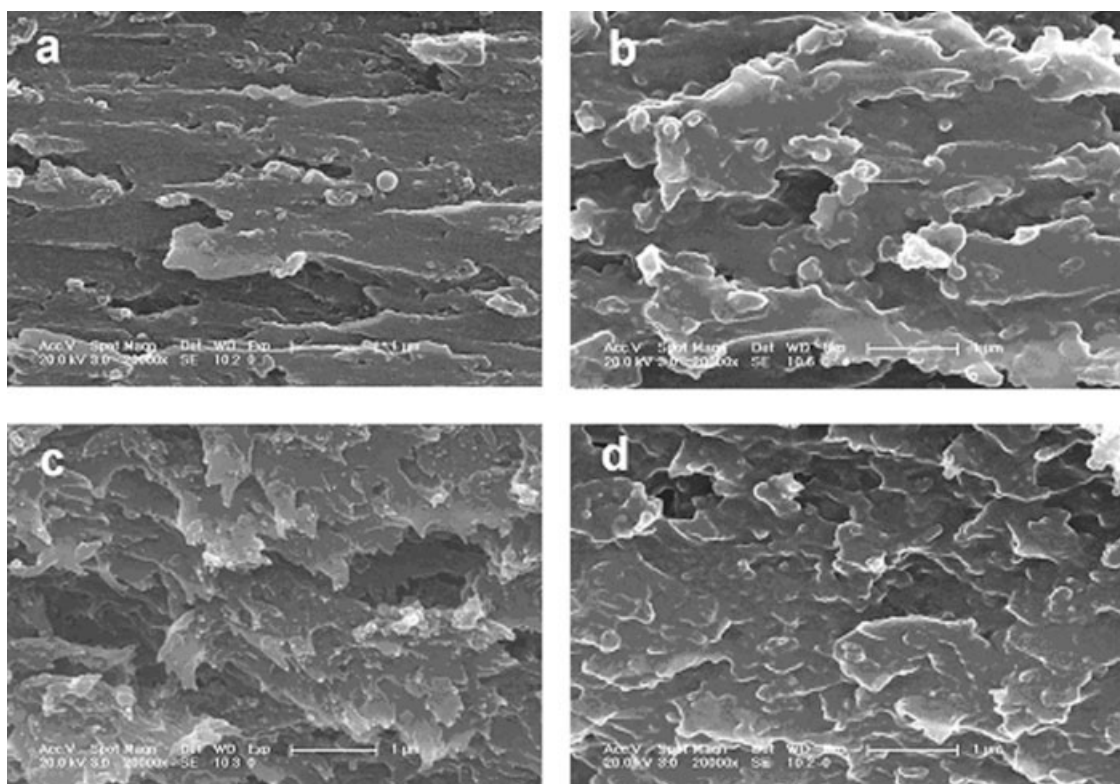


**Figure 8** FESEM images of PI/Al<sub>2</sub>O<sub>3</sub> hybrid films with different Al<sub>2</sub>O<sub>3</sub> content (a) 2.5%, (b) 10%, (c) 12.5%, (d) 15%.

pure polyimide film and Figure 7(b,c) is 5 and 15% Al<sub>2</sub>O<sub>3</sub> hybrid films, respectively. The characteristic peaks of symmetric C=O stretching and asymmetric C=O stretching of the imide group are visible at 1776 and 1712 cm<sup>-1</sup>, which are not sensitive to inorganic component. The bending vibration of C=O appears at 725 cm<sup>-1</sup>, and the assignment of the stretching of the imide ring is at 1374 cm<sup>-1</sup>.<sup>36</sup> Obviously, a broad absorption appears at 3200–3700 cm<sup>-1</sup> after hybridization, which are characteristic stretch-

ing vibration and deformation vibration of hydroxylate (O–H from hydrated Al<sub>2</sub>O<sub>3</sub> and absorbed water molecules. After hybridization, the band in 600–1000 cm<sup>-1</sup> become broadening, intensity at 917 cm<sup>-1</sup> becomes stronger while peaks at 800 and 938 cm<sup>-1</sup> become very weak. It is due to the incorporation of Al<sub>2</sub>O<sub>3</sub> nanoparticles in PI matrix.<sup>37</sup>

To investigate the morphology of the PI/Al<sub>2</sub>O<sub>3</sub> hybrids, the casting films were quenched in liquid nitrogen and then broken to obtain fracture surfaces.

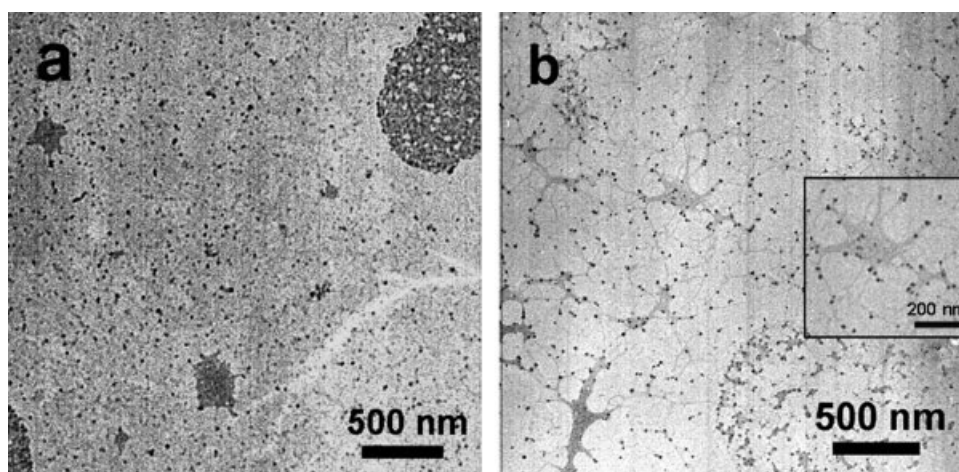


**Figure 9** TEM images of PI/Al<sub>2</sub>O<sub>3</sub> hybrid films with different Al<sub>2</sub>O<sub>3</sub> content (a) 12.5%, (b) 15%, a magnification picture was inserted in the black frame.



Figure 8 shows the FESEM photographs of the fracture surfaces of such hybrid films with different  $\text{Al}_2\text{O}_3$  content. By comparison of four samples, it can be observed that the dispersion of the  $\text{Al}_2\text{O}_3$  particles in the films becomes more even with the  $\text{Al}_2\text{O}_3$  content increasing. The particle size of  $\text{Al}_2\text{O}_3$  in hybrid films is about 20–30 nm. The morphological structure of the hybrids was also studied by TEM (Fig. 9), and the results were consistent with FESEM results. TEM images reveal that the  $\text{Al}_2\text{O}_3$  particle size is about 20–30 nm. For the sample with 15 wt % of  $\text{Al}_2\text{O}_3$  content, an obvious linked structure between  $\text{Al}_2\text{O}_3$  particles can be found in Figure 9(b). Possibly, such a compact  $\text{Al}_2\text{O}_3$  network can serve as a good scaffold and finally lead to the significant enhancement of properties of hybrid films, such as electrical aging when the  $\text{Al}_2\text{O}_3$  content up to 15 wt %.

### CONCLUSION

Polyimide/ $\text{Al}_2\text{O}_3$  composite films with different  $\text{Al}_2\text{O}_3$  content were prepared by a sol-gel process. The sol particles were successfully dispersed in the PAA solution by means of the ultrasonic treatment and finally the  $\text{Al}_2\text{O}_3$  particles were well dispersed in the polyimide matrix. The hybrid films obtained by this approach exhibited high thermal stability, excellent dimensional stability, fairly good mechanical property and good corona-resistance property by adequate final addition of  $\text{Al}_2\text{O}_3$ . When the  $\text{Al}_2\text{O}_3$  content is 15%, the  $T_g$  of the hybrid films increased about 20–40°C, and the decomposition temperature at 5% weight loss is enhanced to 601°C. In addition, at this content of  $\text{Al}_2\text{O}_3$ , the time to failure in electrical aging at 3 kV is 825 min, which is 55 times longer than that of pure PI film. The hybrid PI film with 15 wt % of  $\text{Al}_2\text{O}_3$  exhibited a significant enhancement, which may be attributed to the formation of a compact  $\text{Al}_2\text{O}_3$  network in the polyimide matrix.

### References

1. Ghosh, M. K.; Mittal, K. L. *Polyimides: Fundamentals and Applications*; Marce Dekker: New York, 1996.
2. Mittal, K. L., Ed. *Polyimides: Synthesis, Characterization and Applications*; Plenum: New York, 1984; Vols. 1, 2.
3. Feger, C. J.; Khojasteh, M. M.; McGrath, J. E., Eds. *Polyimides: Materials, Chemistry and Characterization*; Elsevier Science: Amsterdam, 1989.
4. Wilson, D.; Stenzenberger, H. D.; Hergenrother, P. M., Eds. *Polyimides*; Blackie: Glasgow, 1990.
5. Lupinski, J. H.; Moore, R. S., Eds. *Polymeric Materials for Electronics Packaging and Interconnection*, ACS Symposium Series 407; American Chemical Society: Washington, DC, 1989.
6. Takekoshi, T. *Adv Polym Sci* 1990, 94, 1.
7. Sroog, C. E. *Prog Polym Sci* 1991, 16, 561.
8. Wong, C. P., Ed. *Polymers for Electronic and Photonic Applications*; Academic Press: New York, 1993; p 167.
9. Numata, S.; Miwa, T.; Misawa, Y.; Makino, D.; Imaizumi, J.; Kinjo, N. *Mater Res Soc Symp Proc* 1988, 108, 113.
10. Fay, C. C.; Clair, A. K. S. T. *J Appl Polym Sci* 1998, 69, 2383.
11. Nandi, M.; Conklin, J. A.; Salvati, L., Jr.; Sen, A. A. *Chem Mater* 1991, 3, 201.
12. Mascia, L.; Kioul, A. *Polymer* 1995, 36, 3649.
13. He, Y. Q.; Ping, Y. H. *Mater Chem Phys* 2003, 78, 614.
14. Qiu, W. L.; Luo, Y. J.; Chen, F. T.; Duo, Y. Q.; Tan, H. M. *Polymer* 2003, 44, 5821.
15. Morikawa, A.; Tyoku, Y.; Kakimoto, M. A.; Imai, Y. *Polym J* 1992, 24, 107.
16. Chiang, P. C.; Whang, W. T. *Polymer* 2003, 44, 2249.
17. Hsiue, G. H.; Chen, J. K.; Liu, Y. L. *J Appl Polym Sci* 2000, 76, 1609.
18. Joly, C.; Goizet, S.; Schrotter, J.C.; Sanchez, J., Escoubes, M. *J Membrane Sci* 1997, 130, 63.
19. Morikawa, A.; Iyoku, Y.; Kakimoto, M.; Yami, Y. *J Mater Chem* 1992, 2, 679.
20. Yang, Y.; Zhu, Z.; Qi, Z. *J Funct Mater* 1999, 30, 78.
21. Wu, J.; Yang, S.; Gao, S.; Hu, A.; Liu, J.; Fan, L. *Euro Polym J* 2005, 41, 73.
22. Zhong, J.; Zhang, M.; Jiang, Q.; Zeng, S.; Dong, T.; Cai, B.; Lei, Q. *Mater Lett* 2006, 60, 585.
23. Alexandre, M.; Dubois, P. *Mater Sci Eng* 2000, 28, 1.
24. Jimenez, G.; Ogata, N.; Kawai, H.; Ogihara, T. *J Appl Polym Sci* 1997, 64, 2211.
25. Usudi, A.; Kawasumi, M.; Kojima, Y.; Okada, A.; Kurau, C. T.; Kamigaito, O. *J Mater Res* 1993, 8, 1174.
26. Ronald, G. K.; Chen, Q. Q. *Polymer* 1993, 34, 783.
27. Tyan, H. L.; Leu, C. M.; Wei, K. H. *Chem Mater* 2001, 13, 222.
28. Chang, J. H.; Park, K. M. *Polym Eng Sci* 2001, 41, 2226.
29. Yano, K.; Usuki, A.; Okada, A. *J Polym Sci Part A: Poly Chem* 1997, 35, 2289.
30. Morgan, A. B.; Gilman, J. W.; Jackson, C. L. *Macromolecules* 2001, 34, 2735.
31. Delozier, D. M.; Orwoll, R. A.; Cahoon, J. F.; Johnston, N. J.; Smith, J. G.; Connell, J. W. *Polymer* 2002, 43, 813.
32. Chen, X. H.; Gonsalves, K. E. *J Mater Res* 1997, 12, 1274.
33. Thompson, C. M.; Herring, H. M.; Gates, T. S.; Connell, J. W. *Compos Sci Technol* 2003, 63, 1591.
34. Harris, F. W. In *Polyimides*; Willson, D.; Stenzenberger, H.; Hergenrother, P., Eds.; Blackie: London, 1990; p 1.
35. Draper, R. E.; Jones, G. P.; Rehder, R. H.; Stutt, M. U.S. Pat. 1997, 5,989,702.
36. Tyan, H. L.; Liu, Y. C.; Wei, K. H. *Polymer* 1999, 40, 4877.
37. Shek, C. H.; Lai, J. K. L.; Gy, T. S.; Lin, G. M. *Nanostruct Mater* 1997, 8, 605.